Available online at www.sciencedirect.com
SCIENCE DIRECT®
International Journal of Heat and Mass Transfer 47 (2004) 4439–4448
International Journal of HEAT and MASS TRANSFER
www.elsevier.com/locate/ijhmt

Numerical investigation of laminar natural convection on a heated vertical plate subjected to a periodic oscillation

X.R. Zhang *, S. Maruyama, S. Sakai

Institute of Fluid Science, Tohoku University, Katahira 2-1-1, Aoba-ku, Sendai 980-8577, Japan

Received 27 August 2003; received in revised form 1 March 2004
Available online 3 July 2004

Abstract

Natural-convective heat transfer of oscillating vertical plates is related to industrial and technological applications. In this paper, a numerical study is described of the laminar natural convection on a periodically oscillating vertical flat plate heated at a uniform temperature. The exact solutions for the classical Stoke's problem and the similarity solutions (by Ostrach) are used to verify the numerical formulation. Of particular interest of this paper is the heat transfer characteristics when the oscillatory velocity being close to the flow velocity in the velocity boundary layer under non-oscillation condition. The results show that a two-fold increase in space-time averaged Nusselt number is achieved. And it is found that the heat transfer for the problem under consideration significantly depends on the dimensionless oscillation velocity, a relative size between the oscillation velocity and the flow velocity in the velocity boundary layer of a stationary plate. The effects of the governing parameters on the heat transfer are investigated numerically. The heat transfer enhancement is found to be increased with the dimensionless oscillation frequency, amplitude, the Prandtl number, but decreased with the Grashof number.

Keywords: Oscillatory boundary condition; Natural convection; Heat transfer

1. Introduction

Over the past several decades, the oscillation-induced heat and mass transport phenomena have been investigated by a number of researchers due to its great importance in the fields of bioengineering, ocean engineering, and chemical industrial engineering et al. Theoretical and experimental investigations of the mass transfer of a diffusing substance for laminar oscillatory flows in a tube have been carried out [1–6]. Their researches demonstrated that, the diffusing substance will disperse at rates much higher than suggested on pure molecular diffusion grounds. The mechanism here is the interaction of the cross-stream-dependent viscous velocity distribution and the radially dependent concentration leading to an enhanced diffusion coefficient. The results on the enhanced diffusion in oscillatory viscous laminar flows suggest that a similar phenomenon should occur in heat conduction in view of the mathematical similarity between heat conduction and diffusion. Kurzweg et al. [7–9] confirmed this conjecture and developed new technology for the heat transfer enhancement by sinusoidal oscillation of a fluid, i.e. heat transfer in a pipe connected to hot and cold reservoirs at both ends has been highly enhanced by imposing sinusoidal oscillation. Very large effective axial heat conduction rates, exceeding those possible with heat pipes by several orders of magnitude, were found to be achievable [7]. Their systems have been proposed as "dream pipe". Ozawa and Kawamoto [10] conducted numerical simulation and visualization experiment to investigate the fundamental heat transfer mechanism of the dream pipe. Furthermore, Nishio et al. [11] proposed phase shifted oscillation-controlled heat transport tubes to further increase the thermal conductivity.

* Corresponding author. Tel./fax: +81-22-217-5244.
E-mail address: xrzhang@pixy.ifs.tohoku.ac.jp (X.R. Zhang).

0017-9310/$ - see front matter © 2004 Elsevier Ltd. All rights reserved.
doi:10.1016/j.ijheatmasstransfer.2004.03.030

Nomenclature

A_0	dimensionless oscillation amplitude, Eq. (6)
c_p	specific heat
f	dimensional oscillation frequency
$\mathbf{g}$	gravity vector
Gr	Grashof number, $Gr = \frac{g\beta(T_w - T_\infty)L^3}{v^2}$
$h_{x,t}$	local instantaneous heat transfer coefficient
k	thermal conductivity for fluid
L	plate length
$Nu_{x,t}$	local instantaneous Nusselt number, Eq. (12)
$\overline{N}u_x$	time-averaged local Nusselt number, Eq. (13)
Nu_{x0}	local Nusselt number of a stationary plate
$\overline{N}u_t$	space-averaged instantaneous Nusselt number, Eq. (14)
$\overline{N}u_{t0}$	space-averaged Nusselt number of a stationary plate
$\overline{N}u$	space-time averaged Nusselt number, Eq. (15)
P	dimensional pressure of the fluid
Pr	Prandtl number of the fluid
$q_{x,t}$	local instantaneous convective heat flux
T	dimensional temperature
t	dimensional time
u	dimensional velocity component in the x direction; dimensional oscillation velocity, Eq. (5)
U	dimensionless oscillation velocity, Eq. (11)
u_{max}	the maximum flow velocity in the velocity boundary layer of a stationary plate
v	dimensional velocity component in the y direction
$\mathbf{V}$	dimensional velocity vector
w_0	dimensionless oscillation frequency, Eq. (7)
x	dimensional vertical coordinate; the displacement of oscillation, Eq. (4)
x_0	dimensional oscillation amplitude
X	dimensionless vertical coordinate, Eq. (8)
y	dimensional horizontal coordinate
Y	dimensionless horizontal coordinate, Eq. (8)

Greek symbols

δ_{max}	the maximum thickness of velocity boundary layer of a stationary plate
δ_t	thickness of thermal boundary layer, Eq. (16)
μ	dynamic viscosity
ρ	density
β	volumetric thermal expansion coefficient
v	kinematic viscosity
ϕ	dimensionless time (phase angle), Eq. (9)
θ	dimensionless temperature, Eq. (10)

The obtained heat transfer data in tubes subjected to oscillatory flow have been reported by Walsh et al. [12], Liao et al. [13] and Fusegi [14], which all show significantly enhanced heat transfer. The combination of oscillatory flow and a series of sharp edges in a tube or channel for heat transfer enhancement has already been investigated by Brunold et al. [15], Howes et al. [16], Mackly and Stonestreet [17], Stephens and Mackley [18]. This kind of oscillatory flow promotes chaotic mixing in the tube, of which radial velocity components are significant [15,16]. Mackley and Stonestreet reported that significant heat transfer enhancement can be achieved in tubes with a series of baffles due to oscillatory flows, especially for low net flow Reynolds number and a 30-fold improvement in Nusselt number was achieved [17]. The oscillatory flow and baffles both had to be present to produce this effect. Stephen and Mackley presented heat transfer data obtained from two oscillatory flow methods, the first being the fluid oscillation in which the baffles remain stationary, whereas the second employing oscillating baffles [18]. The energy efficient heat transfer can be obtained for the two situations, due to the mechanisms of vortex interaction.

However, almost all the previous studies were relevant to forced convection. And as far as the authors are aware, no study on the natural convection heat transfer under the conditions of oscillatory flow or oscillatory wall appears to exist in the open literature. In addition, heat transfer of oscillating vertical plates or channels under natural convection conditions has a wide variety of technological applications. For example, the upwelling flow of deep seawater using the perpetual salt fountain is a kind of natural convection produced by the temperature and salinity differences between the seawater inside and outside a pipe [19]. The upwelling velocity was strongly dependent on the heat transfer between the pipe wall and the deep seawater in the pipe, which is significantly enhanced by the oscillation of pipe wall due to wave motion [20,21].

As the first step of a fundamental understanding and estimation of the heat transfer characteristics of the natural convection under the oscillating-wall conditions, in this paper, numerical investigations using a simple geometrical configuration—a vertical flat plate and laminar flow were conducted. The vertical plate is heated at a constant temperature. And the validity of the sim-

ulation is examined through comparison with the theoretical results of the natural convection under non-oscillation condition and the exact solutions of the classical Stoke's problem. The present investigation mainly attempts to shed light on the oscillation-induced heat transfer enhancement under such an oscillation conditions that the oscillatory velocity and amplitude are respectively close to the flow velocity in the boundary layer and the thickness of velocity boundary layer under non-oscillation condition. In addition, the effects of governing parameters for the problem under consideration on the heat transfer are presented, such as oscillation frequency, amplitude and the Prandtl number.

2. Formulation of numerical model

2.1. Mathematical formulation

Consider a vertical flat plate of length L oscillating sinusoidally within a viscous fluid, as shown schematically in Fig. 1. A zero-thickness plate is assumed in the simulation, at time $t \leqslant 0$, the plate is assumed to be at rest and the fluid is assumed to be at the temperature T_∞ and the fluid is still. For time $t > 0$ the plate temperature is suddenly raised to a higher constant temperature T_w than the surrounding fluid T_∞, and the plate starts moving in its own plane. Choose a Cartesian co-ordinate system with x-axis along the moving plate in the upward direction and y-axis perpendicular to it. The resultant density difference in the presence of a gravitational field causes the fluid to rise. It is assumed that $(T_w - T_\infty)$ is sufficiently small that the Boussinesq approximation can be made. It is also assumed that all over relevant thermodynamic and transport properties are independent of temperature and that compressibility and dissipation effects can be neglected. The subsequent fluid motion can be described by the following governing equations:

$$\nabla \cdot (\rho \mathbf{V}) = 0, \tag{1}$$

$$\frac{\partial(\rho \mathbf{V})}{\partial t} + \nabla \cdot (\rho \mathbf{V}\mathbf{V}) = \mu \nabla^2 \mathbf{V} - \nabla P + \rho \mathbf{g}, \tag{2}$$

$$\frac{\partial(\rho T)}{\partial t} + \nabla \cdot (\rho \mathbf{V} T) = \frac{k}{c_p} \nabla^2 T. \tag{3}$$

The domain of interest is a two-dimensional rectangular geometry in which the plate is kept in the center. The dimensions of height and width for the geometry are respectively set seven and four times of the plate length, as wide as enough to simulate the flow and heat transfer in the case of the plate oscillating within an unbounded viscous fluid. The left and right side walls of the geometry are specified with uniform temperature T_∞, and the top and bottom horizontal walls are assumed to be adiabatic. The velocity boundary conditions considered here are the non-slip conditions on all the solid walls. The plate motion is governed by the time-dependent equations, in which the displacement of oscillation and the oscillatory velocity are in forms of

$$x = x_0 \sin(2\pi f t), \tag{4}$$

$$u = u_0 \cos(2\pi f t) = 2\pi f x_0 \cos(2\pi f t). \tag{5}$$

This oscillation boundary condition is governed by such two dimensionless parameters:

$$A_0 = x_0/\delta_{\max}, \tag{6}$$

$$w_0 = \delta_{\max}/\sqrt{\upsilon/\pi f}, \tag{7}$$

where A_0 is the dimensionless oscillation amplitude, which represents a ratio of the oscillation amplitude to the maximum of velocity boundary layer thickness of a stationary plate. w_0 is the dimensionless oscillation frequency, which describes a comparison of the velocity boundary layer thickness between non-oscillation and oscillation condition. The value of $\sqrt{\upsilon/\pi f}$ approximately corresponds to the thickness of the velocity boundary layer of an oscillating plate [22].

In addition, the dimensionless coordinate, time, temperature and oscillation velocity are defined as

$$X = x/L,\ Y = y/\sqrt{\upsilon/\pi f}, \tag{8}$$

$$\phi = 2\pi f t, \tag{9}$$

$$\theta = (T - T_\infty)/(T_w - T_\infty), \tag{10}$$

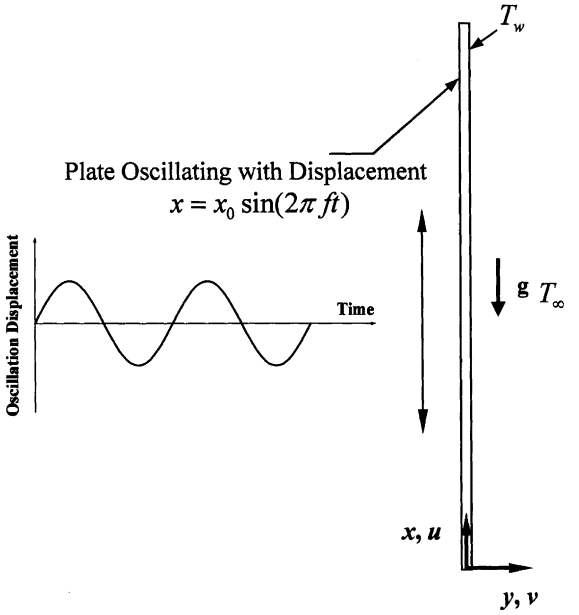

Fig. 1. Schematic diagram of oscillating-plate problem.

$$U = \frac{2\pi f x_0}{u_{\max}}, \tag{11}$$

where U represents a ratio of the oscillation velocity to the maximum flow velocity in the velocity boundary layer of a stationary plate.

The oscillating-wall boundary conditions defined in Eqs. (4) and (5) need to be specified for the concrete case of interest. In this paper, only such an oscillation condition is mainly investigated as the oscillatory velocity and amplitude being respectively less than and close to the flow velocity and the thickness of velocity boundary layer under non-oscillation condition. Therefore, the oscillation amplitude and velocity are respectively limited to $A_0 \leqslant 1$ and $U \leqslant 1$.

The definition of local instantaneous Nusselt number along the heated plate is given as follows:

$$Nu_{x,t} = \frac{h_{x,t}L}{k} = \frac{q_{x,t}L}{(T_w - T_\infty)k}. \tag{12}$$

It should be noted that the value of $Nu_{x,t}$ is a function of the plate location and time. For the purpose of generalizing the spatially and temporally averaged heat transfer data, based on the time and area weighted average of a quantity, the time-averaged local Nusselt number $\overline{N}u_x$, the space-averaged instantaneous Nusselt number $\overline{N}u_t$, and the space-time averaged Nusselt number $\overline{N}u$ can be defined respectively as

$$\overline{N}u_x = \frac{1}{2\pi}\int_0^{2\pi} Nu_{x,t}\,\mathrm{d}\phi, \tag{13}$$

$$\overline{N}u_t = \frac{1}{L}\int_0^{L} Nu_{x,t}\,\mathrm{d}x, \tag{14}$$

$$\overline{N}u = \frac{1}{2\pi L}\int_0^{2\pi}\int_0^{L} Nu_{x,t}\,\mathrm{d}x\,\mathrm{d}\phi. \tag{15}$$

2.2. Method of solution

A finite-volume numerical solution technique based on integration over the control volume is used to solve the model equations (1)–(3) subject to the appropriate boundary conditions. This numerical technique is essentially based on the previous work [23]. A structured non-uniform grid arrangement was employed to solve the discretized equations. The grid was made finer towards the plate wall in order to model accurately the solution variables with large gradients in the near-wall region and capture adequately solutions under the oscillation conditions. Because of the extremely thin velocity and thermal boundary layer at a high dimensionless oscillation frequency, a highly non-uniform grid was deployed. The corresponding grid independence of the results was established by employing various number of mesh points, ranging from 35,000 to 150,000. The time step independence of the solutions was tested, and the typical implicit time step used is 0.01 s, which was chosen as the uppermost value on balance of convergence and CPU time. All the computations in this paper were carried out on the SGI Origin2000 workstation in the Advanced Fluid Information Research Center at Tohoku University, Japan.

2.3. Validation of numerical solution

The formulation of numerical model above is expected to have a capability of reasonably dealing with the laminar natural convection under an oscillating-wall boundary condition. Therefore, for validation of the proposed numerical model, the similarity solutions by Ostrach [24] and the exact solutions for the classical Stoke's second problem [22] were used. A uniform temperature boundary condition is applied on the plate wall when using Ostrach's solution, which describe the velocity and temperature field of buoyant convection on

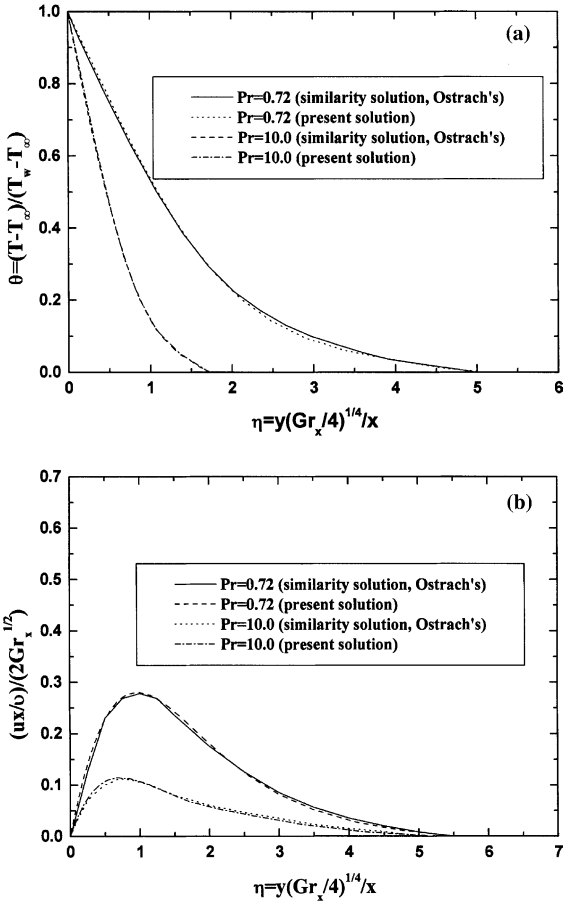

Fig. 2. Comparison of computed dimensionless results with the similarity solution of Ostrach: (a) dimensionless temperature; (b) dimensionless velocity.

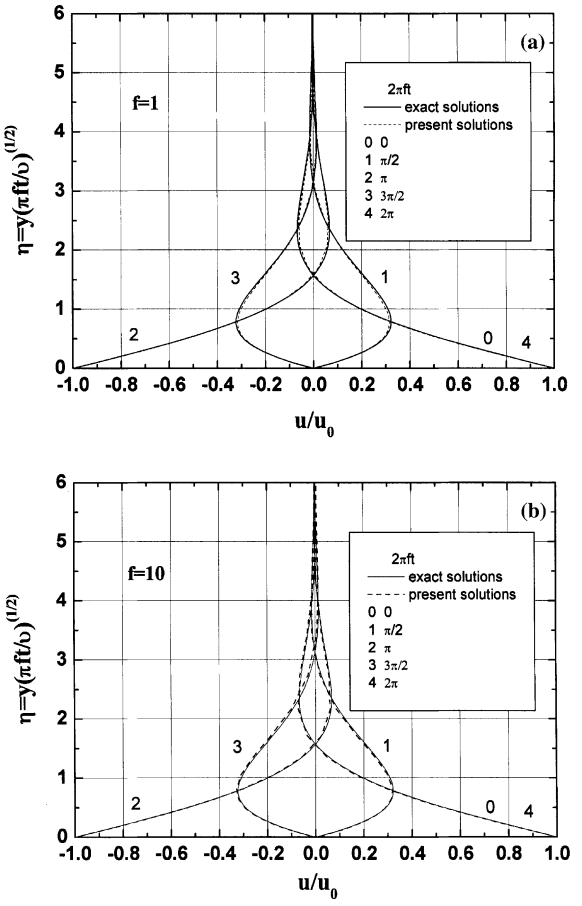

Fig. 3. Comparison of velocity distribution in the neighbourhood of an oscillating plate obtained from validation calculation against the Classic Stokes's second problem: (a) $f = 1$, (b) $f = 10$.

a stationary vertical plate. A moving boundary condition $u = u_0 \cos(2\pi ft)$ was used to compare with the exact solutions for the Stoke's problem, in which the flow solutions about a flat plate which executes linear harmonic oscillations parallel to itself are given. In the geometry described above, air ($Pr = 0.7$) and water ($Pr = 10$) were used as comprehensive validation efforts. The computed solutions are shown in Figs. 2 and 3. The agreement is considered to be acceptable, and therefore the present model can be used with confidence.

3. Results and discussion

An examination of the governing equations and boundary conditions shows that the governing parameters for the problem under consideration are the dimensionless oscillation frequency w_0 and amplitude A_0, the Grashof number Gr (including two parameters, the temperature difference between the plate and ambient fluid and the plate length), and the Prandtl number of fluid Pr. In order to study the effects of the parameters on the heat transfer characteristics, numerical calculations are carried out for a wide range of various parameters. But the parameters for the numerical treatment are chosen in such a way that the Grashof number is less enough than the critical value for the onset of turbulence, and that the magnitude of oscillation velocity is similar to the flow velocity in velocity boundary layer of a stationary plate. In this work, the results of plate length ranging from 0.1 to 0.5 m, oscillation frequency from 0.2 to 10.0 Hz, amplitude from 0.002 to 0.1 m and temperature difference from 0.2 to 20 °C are presented. The numerical simulations were mainly performed for a laminar flow of air ($Pr = 0.7$).

In the present study, the main concern is focused on the case of the oscillation velocity and amplitude close to the flow velocity and the thickness of the velocity boundary layer of a stationary plate. A comparison of the space-time averaged Nusselt number for $U = 0.9$ and for a stationary plate at $Gr = 3 \times 10^7$ are shown in Fig. 4. Fig. 4 is for the value of w_0 from 18.0 to 80.0 and corresponding oscillation amplitude A_0 from 0.9 to 0.04, which exactly falls to the range of the oscillation boundary condition described above. The results show that a two-fold increase in the space-time averaged Nusselt number is achieved (relative to the average Nusselt number of a stationary plate) under such an oscillation boundary condition. Fig. 4 also shows that, at a maintained oscillation velocity ($U = 0.9$), the space-time averaged Nusselt numbers only decrease a little with the frequency w_0. The oscillation amplitude drops rapidly with the increase of frequency at a fixed oscillation velocity, which may lead to such a change of the average Nusselt number as shown in Fig. 4.

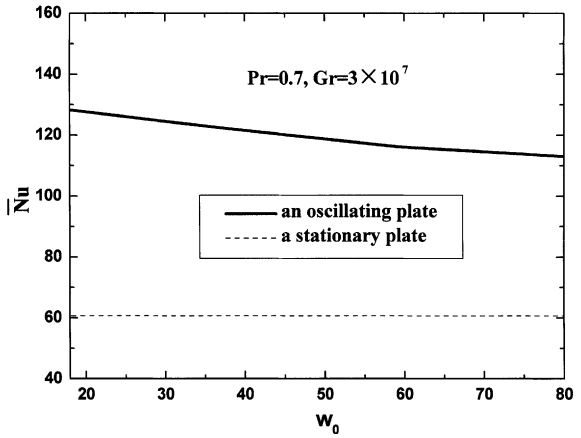

Fig. 4. Comparison of the space-time averaged Nusselt number between a stationary plate and an oscillating plate at a fixed velocity ($U = 0.9$) for $Pr = 0.7$ and $Gr = 3 \times 10^7$.

At the fixed oscillation velocity ($U = 0.9$), the variations of the space-averaged instantaneous Nusselt number $\overline{N}u_t$ and the local instantaneous Nusselt number $Nu_{x,t}$ at different dimensionless locations of the plate during one-cycle for $w_0 = 18.0$ and $A_0 = 0.9$ are respectively given in Fig. 5(a) and (b). Comparing the two $\overline{N}u_t$ curves in Fig. 5(a), it is seen that the space-averaged instantaneous heat transfer can be enhanced greatly throughout all the time of the whole cycle. In this case, the value of w_0 is 18.0, according to the physical meaning of w_0, implying that the thermal boundary thickness becomes thinner than that of a stationary plate due to such an oscillating wall, which maybe contribute to the heat transfer enhancement. Fig. 5(a) also illustrates the change of $\overline{N}u_t$ with time throughout the full cycle. During per oscillation cycle, $\overline{N}u_t$ decreases with phase angle ϕ until it reaches a minimum value around $\phi = 90$. And then $\overline{N}u_t$ begins to increase after $\phi > 90$ to a maximum value around $\phi = 270$. After $\phi > 270$, $\overline{N}u_t$ decreases gradually again to the same value at the beginning of the cycle, which implies a converged solution. It can be seen that the variation of $\overline{N}u_t$ in one-cycle is almost reversely symmetric with respect to $\phi = 180$.

Fig. 5(b) demonstrates the time variation trends of Nusselt number in a complete cycle, from the bottom side to the top side of the plate. At each location, $Nu_{x,t}$ changes with phase angle ϕ with a maximum value (peak) and a minimum value (valley) during one-cycle. And the closer to the two ends of the plate, the greater the variation amplitude of the Nusselt number during one-cycle is. Toward the middle of the plate, the time-variation amplitude for $Nu_{x,t}$ becomes vanishingly small. It can be physically explained that the boundary layer thickness of the middle part of the plate is more difficult to be changed with time than that of the two end parts of the plate. Fig. 5(b) also demonstrates that the heat transfer at the top part of the plate is greatly increased, which even exceeds those at lower locations of the plate.

The results for the space-time averaged Nusselt numbers under a wide range of the oscillation velocities U are shown in Fig. 6. It can be seen that the average Nusselt number increases with the value of U. When the oscillation velocity u_0 is about ten times larger than the magnitude of fluid flow velocity $u_{\max}$ of a stationary plate, about six-fold increase in the average Nusselt number is observed. Even when u_0 is the one-tenth of the value of $u_{\max}$, about 10% increase over the non-oscillatory heat transfer can be achieved. Therefore, by imposing an oscillatory motion on the plate under the buoyant convection, heat transfer performance is kept at a high level. Moreover, heat transfer depends significantly on the dimensionless oscillation velocity U imposed. Regulating the frequency and amplitude under the certain buoyant convection, the heat transfer performance can be brought to a predetermined level.

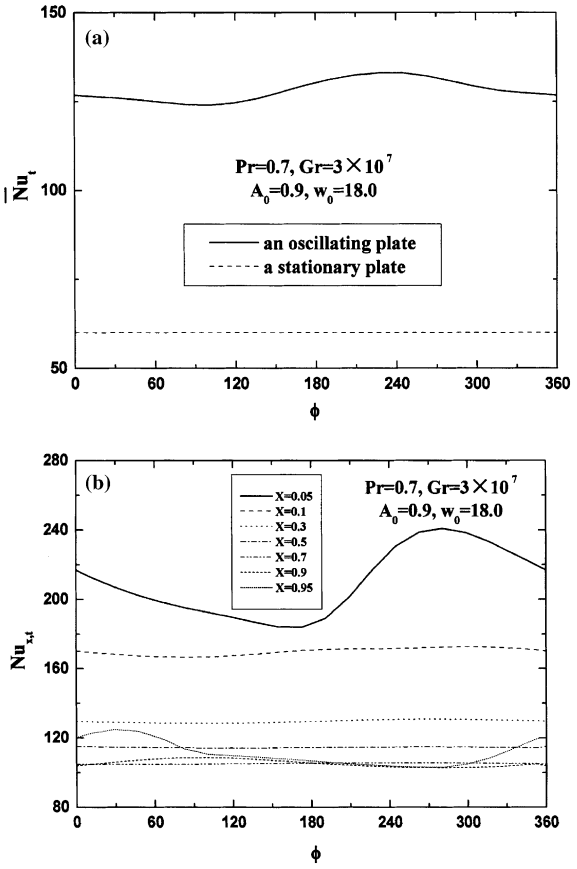

Fig. 5. Variations of Nusselt number during one oscillation cycle for $Pr = 0.7$, $Gr = 3 \times 10^7$, $A_0 = 0.9$ and $w_0 = 18.0$: (a) the space-averaged instantaneous Nusselt number; (b) the local instantaneous Nusselt number along the plate.

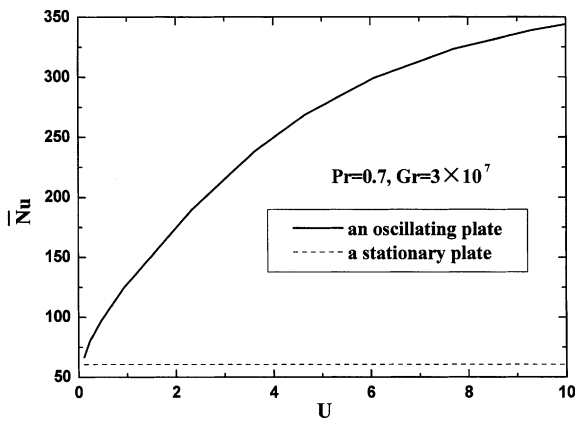

Fig. 6. Variation of the space-time averaged Nusselt number with the dimensionless oscillation velocity (U) for $Pr = 0.7$ and $Gr = 3 \times 10^7$.

The effects of the dimensionless frequency w_0 and amplitude A_0 on the space-averaged instantaneous Nusselt number $\overline{N}u_t$ and the time-averaged local Nusselt number $\overline{N}u_x$ for $G = 3 \times 10^7$ are shown in Fig. 7(a) and (b). A comparison of case 1 ($A_0 = 0.9$ and $w_0 = 18.0$) and case 2 ($A_0 = 0.9$ and $w_0 = 14.0$) shows that $\overline{N}u_t$ and $\overline{N}u_x$ increase with the increase of w_0 at a fixed value of A_0, which implies that the heat transfer rate increase with the increase of frequency at a fixed oscillation amplitude of the plate. This is because the thickness of thermal boundary layer in an oscillatory condition is given as [10]

$$\delta_t = \sqrt{\upsilon/\pi f}/Pr, \tag{16}$$

which implies that the thickness becomes thinner with w_0. Consequently, the heat transfer rate increases with the value of w_0. Similarly, a comparison of case 1 ($A_0 = 0.9$ and $w_0 = 18.0$) and case 3 ($A_0 = 0.45$ and $w_0 = 18.0$) shows that the values of $\overline{N}u_t$ and $\overline{N}u_x$ increase with the increase of A_0 at a fixed value of w_0, which implies that the heat transfer rate increases with the increase of oscillation amplitude at a fixed value of frequency. This can be explained based on the energy Eq. (3). With fixed values of w_0 and physical properties of the fluid, the convection term in Eq. (3) becomes more significant with the increasing value of A_0. Physically, a higher value of A_0 means the plate is subjected to a stronger convection during each cycle.

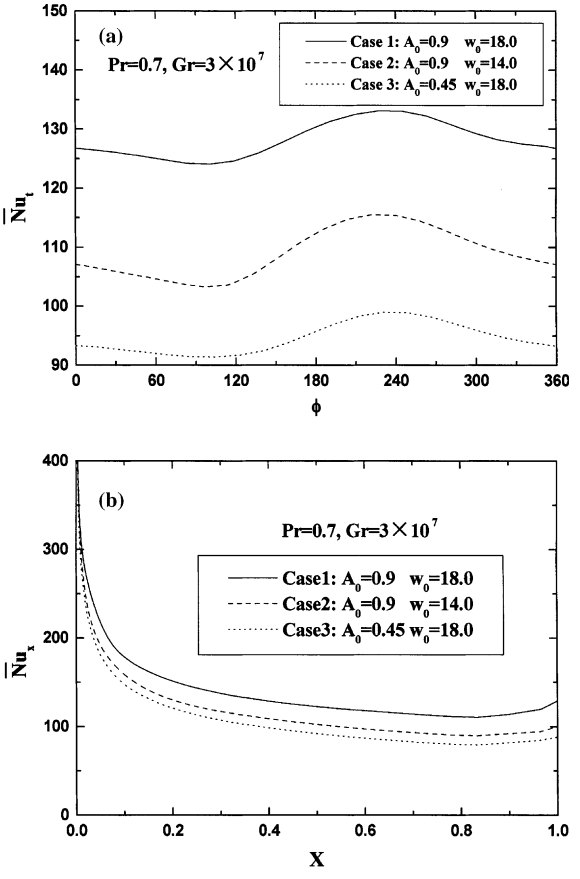

Fig. 7. Effect of the dimensionless oscillation frequency (w_0) and amplitude (A_0) on the space-averaged instantaneous Nusselt number ($\overline{N}u_t$) and the time-averaged local Nusselt number $\overline{N}u_x$ for $Pr = 0.7$ and $Gr = 3 \times 10^7$.

Transient temperature profiles during a complete cycle under different oscillation frequency and amplitude are presented in Fig. 8(a)–(c). Heat transfer rate is directly relevant to the temperature profiles, which change with phase angle all the time through a whole cycle. A comparison of the temperature profiles between Fig. 8(a) and (b) shows that temperature gradients near the plate become steeper when the value of w_0 is increased, which implies that the heat transfer is enhanced with the increase of the dimensionless oscillation frequency for a fixed value of oscillation amplitude. If w_0 is fixed and A_0 is increased, the convection term in Eq. (3) will become larger and will have some effect on the temperature profile. This point is illustrated in a comparison of Fig. 8(a) and (c) that the temperature gradient near the plate becomes larger under a higher oscillation amplitude.

The effect of the Grashof number (the temperature difference is changed at a fixed plate length) on the time-averaged local Nusselt number $\overline{N}u_x$ for $A_0 = 0.9$ and $w_0 = 16.0$ (the value of δ_{max} at $Gr = 3 \times 10^7$ is used as the reference value when deriving A_0 and w_0) is shown in Fig. 9, in which the ratios of the heat transfer (the value of $\overline{N}u_x$) of the oscillation condition and non-oscillation condition for three buoyant force at a fixed frequency and amplitude are illustrated. It can be seen that the ratios increase with the decrease of Grashof number. At the fixed oscillation frequency and amplitude, under a smaller buoyant force, a higher heat transfer enhancement is obtained. The reason given for this behavior is that the ratio of the oscillation velocity u_0 and the flow velocity u_{max} in the boundary layer under non-oscillation condition becomes smaller and smaller with the increase of the temperature difference. In Fig. 9, corresponding to the three Grashof number, 3×10^6, 3×10^7 and 3×10^8, the ratios of u_0 and u_{max} are 3.45, 0.80 and 0.25, respectively. As described in Fig. 6, the heat transfer enhancement by an oscillating-wall condition is appreciably related to the relative size of the value of u_0 and u_{max}. Therefore, at a fixed oscillation velocity, the heat transfer performance can be kept at a higher level for a smaller buoyancy force. This phenomena is similar to the conclusion shown in the research of forced convection [17], in which the greater advantage for the heat transfer enhancement of oscillatory flow appears to be found at low net flow Reynolds number.

The effect of the Grashof number (the plate length is changed at a fixed temperature difference) on the

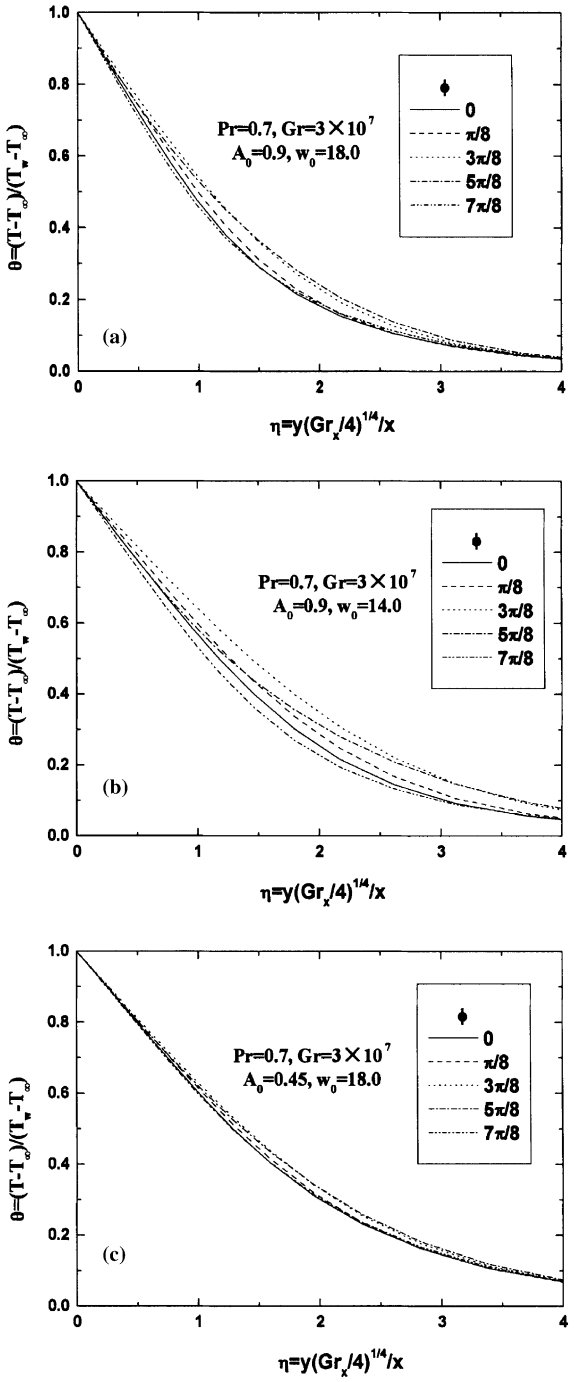

Fig. 8. Evolutions of the temperature profile (θ) during one oscillation cycle for $Pr = 0.7$ and $Gr = 3 \times 10^7$. (a) $A_0 = 0.9$, $w_0 = 18.0$; (b) $A_0 = 0.9$, $w_0 = 14.0$; (c) $A_0 = 0.45$, $w_0 = 18.0$.

time-averaged local heat transfer coefficient $\bar{h}_x$ for $A_0 = 0.9$ and $w_0 = 18.0$ (the value of $\delta_{\max}$ at L_1 is used as the reference value when deriving A_0 and w_0) is shown in

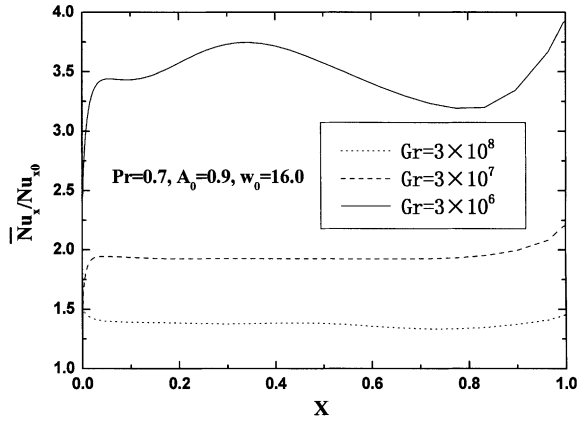

Fig. 9. Effect of the Grashof number on the time-averaged local Nusselt number for $Pr = 0.7$, $A_0 = 0.9$ and $w_0 = 16.0$.

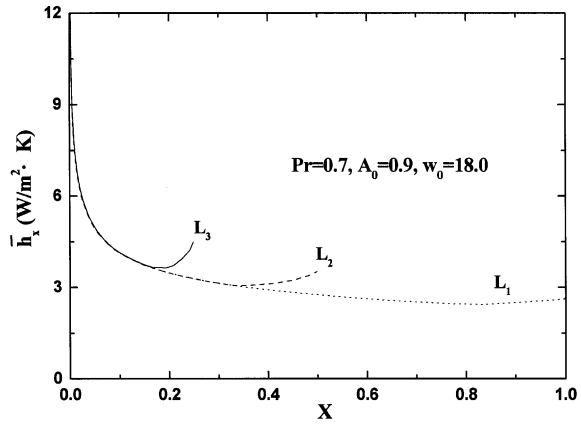

Fig. 10. Effect of the plate length on the time-averaged local heat transfer coefficient for $Pr = 0.7$, $A_0 = 0.9$ and $w_0 = 18.0$ ($L_3/L_1 = 0.25$, $L_2/L_1 = 0.5$).

Fig. 10, in which X represents the ratio of the local x coordinate and the longest plate length L_1. As shown in this figure, when the plate length increases from L_3 (0.25 L_1) to L_1, the time-averaged local heat transfer coefficient in the bottom regions of the plates remains the same value while those in the top regions increase with the decrease of the plate length. Physically, the decrease of the plate length at a fixed A_0 and w_0 means that the ratio of the oscillation amplitude to the plate length becomes larger, which lead to such a higher space-time averaged Nusselt number for a shorter plate.

The effect of the Prandtl number of the fluid on the space-averaged instantaneous Nusselt number $\overline{Nu}_t$ during a complete cycle is shown in Fig. 11. The values of Pr are taken as 0.7 and 10.0 which physically corresponds to air and water, respectively. Fig. 11 illustrates the ratios of $\overline{Nu}_t$ of an oscillatory plate and a stationary plate

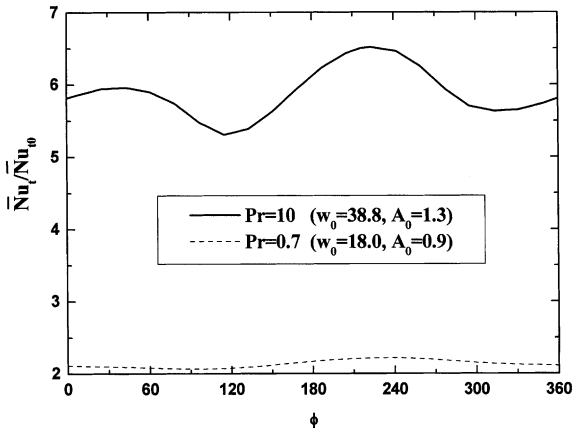

Fig. 11. Effect of the Prandtl number of the fluid on the space-averaged instantaneous Nusselt number during one oscillation cycle.

for air and water. The results show that a six-fold increase in the average Nusselt number is achieved for water, much larger than the ratio of air at the same oscillation frequency and amplitude. In the case of Fig. 11, the dimensionless oscillation amplitude A_0 are 0.9 and 1.3 for air and water, however, the values of w_0 for water is 38.8, two times larger than 18.0, that of air (because of the kinematic viscosity of water being much less than that of air), which implies that, the thickness of thermal boundary layer for water is appreciably decreased larger than that using air as the working fluid. Therefore, a higher heat transfer enhancement can be achieved by using the fluid of larger Prandtl number under a fixed oscillation boundary condition.

4. Concluding remarks

A numerical solution of the governing equations for laminar natural convection on an periodically oscillating plate has been presented. The following remarks are made from the results of this study:

(1) Comparison of the existing theoretical data (the exact solutions of the classical Stoke's problem of a sinusoidally oscillating flat plate immersed within a viscous fluid and the similarity solutions for laminar natural convection on a stationary vertical plate) and model prediction validates the model for reasonably predicting laminar natural-convective flow and heat transfer in the case of a vertical plate subjected to a periodic oscillation.

(2) This paper focuses on the investigation of heat transfer characteristics under such an oscillation condition as the magnitude of oscillation velocity close to the flow velocity in the velocity boundary layer of a stationary plate. The results show that a two-fold increase in the space-time averaged Nusselt number is obtained.

(3) The heat transfer performance of an oscillation plate depends significantly on the dimensionless oscillation velocity, which represents a relative size between the oscillation velocity and the flow velocity in the velocity boundary layer of a stationary plate. The larger the dimensionless oscillation velocity, the higher heat transfer can be achieved.

(4) The problem considered is governed by the following independent parameters, the dimensionless oscillation frequency w_0 and amplitude A_0, the Grashof number Gr (including temperature difference ΔT and plate length L), and the Prandtl number of fluid Pr. The results reveal that the heat transfer enhancement is increased with the increase of the frequency w_0, the amplitude A_0 and the Prandtl number Pr, but decreased with the increase of temperature difference ΔT and plate length L.

References

[1] G.I. Taylor, Dispersion of soluble matter in solvent flowing slowly through a tube, Proc. Royal Soc. Lond. 219 (1953) 186–203.
[2] P.C. Chatwin, On the longitudinal dispersion of passive contaminant in oscillatory flows in tubes, J. Fluid Mech. 71 (1975) 513–527.
[3] R. Smith, Contaminant dispersion in oscillatory flows, J. Fluid Mech. 114 (1982) 379–398.
[4] E.J. Watson, Diffusion in oscillatory pipe flow, J. Fluid Mech. 133 (1983) 233–244.
[5] C.H. Joshi, R.D. Kamm, J.M. Drazen, A.S. Slutsky, An experimental study of gas exchange in laminar oscillatory flow, J. Fluid Mech. 133 (1983) 245–254.
[6] M.J. Jaeger, U.H. Kurzweg, Determination of the longitudinal dispersion coefficient in flows subjected to high-frequency oscillations, Phys. Fluids 26 (1983) 1380–1382.
[7] U.H. Kurzweg, L.D. Zhao, Heat transfer by high frequency oscillations: a new hydrodynamic technique for achieving large effective thermal conductivities, Phys. Fluids 27 (1984) 2624–2627.
[8] U.H. Kurzweg, Enhanced heat conduction in fluids subjected to sinusoidal oscillations, Trans. ASME, J. Heat Transfer 107 (1985) 459–462.
[9] U.H. Kurzweg, Temporal and spatial distribution of heat flux in oscillating flow subjected to an axial temperature gradient, Int. J. Heat Mass Transfer 29 (1986) 1969–1977.
[10] M. Ozawa, A. Kawamoto, Lumped-parameter modeling of heat transfer enhanced by sinusoidal motion of fluid, Int. J. Heat Mass Transfer 34 (1991) 3083–3094.
[11] S. Nishio, X.H. Shi, W.M. Zhang, Oscillation-induced heat transport: heat transport characteristics along liquid-columns of oscillation-controlled heat transport tubes, Int. J. Heat Mass Transfer 38 (1995) 2457–2470.
[12] T.E. Walsh, K.T. Yang, V.W. Nee, Q.D. Liao, Forced convection cooling in microelectronic cabinets via oscillatory flow techniques, Exp. Heat Transfer, Fluid Mech. Thermo. (1993) 641–648.

[13] Q.D. Liao, K.T. Yang, V.W. Nee, Enhanced microprocessor chip cooling by channeled zero-mean oscillatory air flow, Adv. Electron. Packaging 2 (1995) 789–794.
[14] T. Fusegi, Mixed convection in periodic open cavities with oscillatory throughflow, Numer. Heat Transfer, Part A 29 (1996) 33–47.
[15] C.R. Brunold, J.C.B. Hunns, M.R. Mackley, J.W. Thompson, Experimental observations on flow patterns and energy losses for oscillatory flows in ducts with sharp edges, Chem. Engng. Sci. 44 (1989) 1227–1244.
[16] T. Howes, M.R. Mackley, E.P.L. Roberts, The simulation of chaotic mixing and dispersion for periodic flows in baffled channels, Chem. Engng. Sci. 46 (1991) 1669–1677.
[17] M.R. Mackley, P. Stonestreet, Heat Transfer and associated energy dissipation for oscillatory flow in baffled tubes, Chem. Engng. Sci. 50 (1995) 2211–2224.
[18] G.G. Stephens, M.R. Mackley, Heat transfer performance for batch oscillatory flow mixing, Exp. Thermal Fluid Sci. 25 (2002) 583–594.
[19] S. Maruyama, M. Ishikawa, K. Taira, Japanese patent no. 158594, 2000.
[20] S. Maruyama, K. Tsubaki, K. Taira, S. Sakai, Artificial upwelling of deep seawater using the perpetual salt fountain for cultivation of ocean desert, J. Oceanogr. 60 (2004) 563–568.
[21] N. Takahashi, S. Maruyama, S. Sakai, K. Taira, A numerical analysis of natural convection using temperature and concentration differences, Mem. Inst. Fluid Sci., Tohoku University (2002) 21–30.
[22] H. Schlichting, Boundary-Layer Theory, seventh ed., McGraw-Hill, New York, 1979, pp. 93–95.
[23] X.R. Zhang, S. Maruyama, S. Sakai, K. Tsubaki, M. Behnia, Flow prediction in upwelling deep seawater—the perpetual salt fountain, Deep Sea Research Part I: Oceanographic Research Papers, in press.
[24] S. Ostrach, An analysis of laminar free convection flow and heat transfer about a flat plate parallel to the direction of the generating body force, NASA report, 1953, pp. 63–79.